Int. J. Heat Mass Transfer. Vol. 33, No. 10, pp. 2265–2274, 1990
Printed in Great Britain

0017-9310/90 $3.00 + 0.00

Natural convection heat and mass transfer along a vertical cylinder in a porous medium

ADNAN YÜCEL
Mechanical Engineering Department, The University of Texas at Arlington, Arlington, TX 76019, U.S.A.

(*Received* 4 *May* 1989 *and in final form* 2 *January* 1990)

Abstract—Combined heat and mass transfer in natural convection along a vertical cylinder in a saturated porous medium is studied. The boundary layer analysis is formulated in terms of the combined thermal and solutal buoyancy effect. The flow field characteristics are analyzed in detail for both cases where the concentration gradients can either aid or oppose the thermal buoyancy forces. The effects of the curvature, the buoyancy parameter and the Lewis number on the temperature, concentration and flow fields, and on the surface heat and mass transfer rates are discussed.

1. INTRODUCTION

NATURAL convection flows driven by combined thermal and solutal buoyancy forces in a porous medium are encountered in many geophysical and engineering applications. These include moisture transport in thermal insulations, pore water convection near salt domes, movement of contaminants in groundwater, and waste dissolution and release in underground nuclear waste disposal. The majority of studies on natural convection in porous media deal with a single, namely thermal, driving force [1, 2]. Research on buoyant flows arising from combined forces has been directed primarily on the convective instability of porous layers with vertical density gradients [3–5]. Only a few studies have considered the interaction between the thermal and solutal buoyancy effects in porous media subjected to horizontal density gradients. Bejan and Khair [6] presented a scale analysis of heat and mass transfer about a vertical plate in a porous medium. They considered concentration gradients which aid or oppose thermal gradients, but reported limited similarity results for the latter case. Trevisan and Bejan [7] extended the analysis to a porous medium confined between two vertical walls maintained at different temperature and concentration levels. Recently, Evans and Nunn [8] studied combined heat and salt transport in sediments surrounding a salt column. The present study addresses the problem of free convection about a vertical cylinder in a porous medium due to combined driving forces. Natural convection about a vertical plate is a special case of the problem under consideration. The formulation of the problem is based on the combined buoyancy effect, rather than the limiting case of heat—or mass—transfer driven flow. The range of buoyancy parameters and Lewis numbers for which flows are possible are identified for both favorable and adverse solutal density gradients. Numerical results are presented to quantify the transverse curvature effects on the flow, temperature and concentration fields. The problem under consideration has important applications in the study of geological formations; in the exploration and thermal recovery of oil; and in the assessment of aquifers, geothermal reservoirs and underground nuclear waste storage sites. Results obtained from this study will be helpful in the prediction of flow, heat transfer and solute or contaminant dispersion about intrusive bodies such as salt domes, magmatic intrusions, piping and casing systems and similar structures found in these applications [1, 2, 8, 9].

2. ANALYSIS

Consider the problem of steady free convection about a vertical cylinder of radius R in a saturated porous medium at temperature T_∞ and concentration C_∞. The surface of the cylinder is maintained at a uniform temperature T_w and uniform concentration C_w (Fig. 1). Let x and r denote the axial and radial

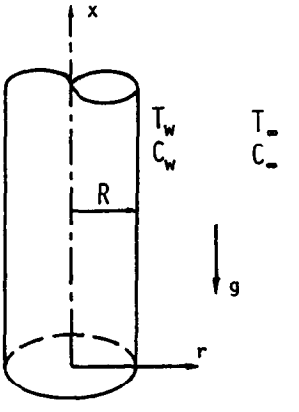

FIG. 1. Schematic diagram of the physical system.

NOMENCLATURE

A	constant defined by equation (15)
AC	aiding case, equations (6), (8) and (19) with the '+' sign
C	concentration
CPR	mass flux ratio defined by equation (30b)
D	equivalent mass diffusivity of the porous medium
f	dimensionless stream function
g	gravitational acceleration
Gr_x	local Grashof number, equation (14)
j	mass flux
K	permeability
Le	Lewis number, α/D
N	buoyancy ratio, equation (17)
Nu_x	local Nusselt number, equation (29a)
OC	opposing case, equations (6), (8) and (19) with the '−' sign
Pr	Prandtl number, ν/α
p	pressure
r	radial coordinate
R	cylinder radius
q	heat flux
Sc	Schmidt number, ν/D
Sh_x	local Sherwood number, equation (29b)
T	temperature
TPR	heat flux ratio defined by equation (30a)
u	axial velocity component
v	radial velocity component
w	buoyancy parameter, equation (16)
x	axial coordinate.

Greek symbols

α	thermal diffusivity
β_C, β_T	absolute values of the coefficients of concentration and thermal expansion
η	transformed radial coordinate
θ	dimensionless temperature
μ	viscosity coefficient
ν	kinematic viscosity coefficient, μ/ρ_∞
ξ	transformed axial coordinate
ρ	density
ϕ	dimensionless concentration
ψ	stream function.

Subscripts

w	quantity at wall
∞	quantity at infinity.

coordinates measured along and from the axis of the cylinder, respectively. In order to reduce the number of independent parameters in the analysis, we use the following conventional assumptions [5]: (1) the porous medium is homogeneous and isotropic, (2) all physical properties are assumed to be constant except for the density in the buoyancy term, which is given by the Boussinesq approximation, (3) the flow is sufficiently slow such that the convective fluid and the porous medium are in local thermodynamic equilibrium and Darcy's law is valid, and (4) the analysis is confined to low-level concentration differences such that the cross diffusion effects and the interfacial velocity at the cylinder surface due to mass diffusion can be neglected.

Under these assumptions, the equations governing the flow, energy and solute transport in cylindrical coordinates are

$$\frac{\partial}{\partial x}(ru)+\frac{\partial}{\partial r}(rv)=0 \tag{1}$$

$$u=-\frac{K}{\mu}\left(\frac{\partial p}{\partial x}+\rho g\right) \tag{2}$$

$$v=-\frac{K}{\mu}\frac{\partial p}{\partial r} \tag{3}$$

$$u\frac{\partial T}{\partial x}+v\frac{\partial T}{\partial r}=\alpha\left[\frac{1}{r}\frac{\partial}{\partial r}\left(r\frac{\partial T}{\partial r}\right)+\frac{\partial^2 T}{\partial x^2}\right] \tag{4}$$

$$u\frac{\partial C}{\partial x}+v\frac{\partial C}{\partial r}=D\left[\frac{1}{r}\frac{\partial}{\partial r}\left(r\frac{\partial C}{\partial r}\right)+\frac{\partial^2 C}{\partial x^2}\right] \tag{5}$$

where u, v, p, T and C are volume-averaged quantities representing respectively the velocity components in the x- and r-directions, pressure, temperature and concentration. The properties ρ and μ are the solution density and viscosity, K is the permeability, and α and D the equivalent thermal and mass diffusivities of the saturated porous medium. The density in the buoyancy term in equation (2) is given by

$$\rho=\rho_\infty\{1-[\beta_T(T-T_\infty)\pm\beta_C(C-C_\infty)]\}. \tag{6}$$

The subscript '∞' denotes the condition at infinity; β_T and β_C are the absolute values of the coefficients of thermal and concentration expansion. The '+' and '−' signs denote cases where the solutal buoyancy effect aids and opposes the thermal buoyancy effect, which are hereafter referred to as the 'aiding case' (AC) and the 'opposing case' (OC), respectively.

The boundary conditions for the problem are

$$v=0,\ T=T_w,\ C=C_w \quad \text{at } r=R \tag{7a}$$

$$u\to 0,\ T\to T_\infty,\ C\to C_\infty \text{ as } r\to\infty. \tag{7b}$$

2.1. *Boundary layer equations*

The boundary layer approximation can be invoked if the Grashof number is so large that the buoyant flow is confined to a thin layer adjacent to the cylinder surface [9, 10]. Under the boundary layer assump-

tions, the governing equations become

$$\frac{\partial}{\partial r}\left(\frac{1}{r}\frac{\partial \psi}{\partial r}\right) = \frac{gK}{\nu}\left(\beta_T \frac{\partial T}{\partial r} \pm \beta_C \frac{\partial C}{\partial r}\right) \tag{8}$$

$$\frac{\partial \psi}{\partial r}\frac{\partial T}{\partial x} - \frac{\partial \psi}{\partial x}\frac{\partial T}{\partial r} = \alpha \frac{\partial}{\partial r}\left(r \frac{\partial T}{\partial r}\right) \tag{9}$$

$$\frac{\partial \psi}{\partial r}\frac{\partial C}{\partial x} - \frac{\partial \psi}{\partial x}\frac{\partial C}{\partial r} = D \frac{\partial}{\partial r}\left(r \frac{\partial C}{\partial r}\right) \tag{10}$$

where ψ is the stream function which automatically satisfies the continuity equation. The velocity components are given by

$$ru = \frac{\partial \psi}{\partial r}, \quad rv = -\frac{\partial \psi}{\partial x}. \tag{11}$$

In order to nondimensionalize the above equations we introduce the pseudo-similarity variable η

$$\eta = (R/2x)(Gr_x/A)^{1/2}[(r/R)^2 - 1] \tag{12}$$

and the non-similarity variable ξ

$$\xi = (2x/R)(A/Gr_x)^{1/2} \tag{13}$$

together with

$$Gr_x = gK[\beta_T(T_w - T_\infty) + \beta_C(C_w - C_\infty)]x/\nu^2 \tag{14}$$

$$A = (1-w)/Pr + w/Sc \tag{15}$$

$$w = [\beta_C(C_w - C_\infty)]/[\beta_T(T_w - T_\infty) + \beta_C(C_w - C_\infty)]. \tag{16}$$

Note that Gr_x, which is the modified local Grashof number for a saturated porous medium, is defined to represent the combined buoyant driving force. The buoyancy parameter w is a measure of the magnitude of the concentration (mass) buoyancy effect relative to the combined thermal and mass buoyancy effect. It is related to the more commonly used 'buoyancy ratio' N by

$$w = N/(N+1), \quad N = [\beta_C(C_w - C_\infty)]/[\beta_T(T_w - T_\infty)]. \tag{17}$$

The buoyancy parameter w varies between 0 and 1. Values of w close to 0 and 1 imply dominant thermal and solutal buoyancy effects, respectively.

The dimensionless stream function f, temperature θ and concentration ϕ are defined by the following relations:

$$\psi(x,y) = \nu R A^{1/2} Gr_x^{1/2} f(\xi,\eta) \tag{18a}$$

$$T(x,y) = T_\infty + (T_w - T_\infty)\theta(\xi,\eta) \tag{18b}$$

$$C(x,y) = C_\infty + (C_w - C_\infty)\phi(\xi,\eta). \tag{18c}$$

Under these transformations, the governing equations and the boundary are cast into the following form:

$$f'' - [(1-w)\theta' \pm w\phi'] = 0 \tag{19}$$

$$\left(\frac{Le}{(1-w)Le + w}\right)[(1+\xi\eta)\theta']' + \tfrac{1}{2}f\theta' + \tfrac{1}{2}\xi\left(\theta'\frac{\partial f}{\partial \xi} - f'\frac{\partial \theta}{\partial \xi}\right) = 0 \tag{20}$$

$$\left(\frac{1}{(1-w)Le + w}\right)[(1+\xi\eta)\phi']' + \tfrac{1}{2}f\phi' + \tfrac{1}{2}\xi\left(\phi'\frac{\partial f}{\partial \xi} - f'\frac{\partial \phi}{\partial \xi}\right) = 0 \tag{21}$$

$$f + \xi\frac{\partial f}{\partial \xi} = 0, \ \theta = 1, \ \phi = 1 \text{ at } \eta = 0 \tag{22a}$$

$$f' \to 0, \ \theta \to 0, \ \phi \to 0 \text{ as } \eta \to \infty \tag{22b}$$

where the prime denotes differentiation with respect to η and Le is the Lewis number: $Le = Sc/Pr \equiv (\nu/D)/(\nu/\alpha) = \alpha/D$. The boundary condition on f in equation (22a) follows from the impermeable boundary condition at the cylinder surface ($v = 0$). It can be integrated over ξ to obtain a simpler expression of the form

$$f(\xi, 0) = 0 \tag{22c}$$

since $f(0,0) = 0$.

For $\xi = 0$, the above equations reduce to those for natural convection about a vertical flat plate. Hence, deviations from $\xi = 0$ measure the effect of transverse curvature. It should be noted that as $R \to \infty$ or for thin boundary layers where r does not differ appreciably from R, the pseudo-similarity variable η given by equation (12) reduces to the corresponding similarity variable for a flat plate, $(Gr_x/A)^{1/2}y/x$, where $y = R - r$.

2.2. *Special cases*

In addition to the curvature effect represented by the parameter ξ, other parameters affecting the flow, temperature and concentration fields in the porous medium are the buoyancy parameter w and the Lewis number Le. Two special cases of these parameters are of particular importance.

(1) $w = 0$ *case and* $w = 1$ *case*. These special cases represent two limiting solutions. For $w = 0$, the above variables and equations reduce to those for purely heat transfer driven flow [9]. For $w = 1$, the equations represent those for flow driven solely by species diffusion. Note that the temperature distribution $\theta(\xi,\eta)$ in the $w = 0$ case and the concentration distribution $\phi(\xi,\eta)$ in the $w = 1$ case are both independent of the Lewis number and identical to each other. As a result, the flow fields in these two cases are also identical and independent of the Lewis number (as will be discussed later, the flow direction may be upward or downward in the latter case depending on the sign of the solutal density gradient in equation (19)). Thus, the flow and temperature fields in the $w = 0$ case (or the flow and concentration fields in the

$w = 1$ case) represent the 'base case' solutions in this study.

(2) *$Le = 1$ case.* The Lewis number is a measure of the relative thickness of the thermal boundary layer compared to the concentration boundary layer. When the Lewis number is unity, thermal and mass diffusivities or length scales are equal to each other; thus the temperature distribution $\theta(\xi, \eta)$ is identical to the concentration distribution $\phi(\xi, \eta)$ under the specified boundary conditions. This holds for any value of the buoyancy parameter w (note that equations (20) and (21) are independent of w when $Le = 1$). Consequently, it is seen from equation (19) that the flow field is also independent of w but in the aiding case only. Hence, the flow fields (for the aiding case) and the temperature—or concentration—fields (for both the aiding and opposing cases) when $Le = 1$ also represent the 'base case' solutions discussed above, i.e. they are respectively identical to the flow and temperature fields for the case $w = 0$ for any Le value (or to the flow and concentration fields for the case $w = 1$ for any Le value).

3. FLOW FIELD CHARACTERISTICS

It is important to distinguish between the two cases in which the solutal buoyancy effect either aids or opposes the thermal buoyancy effect in the analysis of the resultant flow. For simplicity, the results and discussion in this paper are limited to physical situations with $T_w > T_\infty$ and $C_w > C_\infty$.

(1) *Aiding case*

The resulting flow in this case is upward as both the temperature and concentration variations impose favorable density differences (equation (6) with the + sign). This can be shown mathematically by integrating equation (19) to obtain

$$f'(\xi, \eta) = (1-w)\theta(\xi, \eta) + w\phi(\xi, \eta). \tag{23}$$

Note that the velocity component in the axial direction is proportional to f'

$$u = u_r f', \quad u_r = gK[\beta_T(T_w - T_\infty) + \beta_C(C_w - C_\infty)]/\nu.$$

Since the temperature θ and concentration ϕ are positive everywhere, f' and consequently u are also positive everywhere. This is true for any value of the Lewis number Le and the buoyancy parameter w. We also note that evaluating equation (23) at $\eta = 0$ shows that $u = u_r$ at the surface, i.e.

$$f'(\xi, 0) \equiv 1 \tag{24}$$

regardless of Le or w.

(2) *Opposing case*

The resulting flow in this case can be upward or downward depending on the relative strength of the adverse buoyancy effect due to concentration (equation (6) with the − sign). For clarity, the following discussion is limited to upward (positive everywhere) flows, but it can be readily extended to downward flows as will be discussed in Section 4.

Integration of equation (19) results

$$f'(\xi, \eta) = (1-w)\theta(\xi, \eta) - w\phi(\xi, \eta) \tag{25}$$

with

$$f'(\xi, 0) = 1 - 2w. \tag{26}$$

Note that the velocity at the surface becomes negative for $w > 1/2$ indicating flow reversal at the surface. Therefore, upward boundary layer flows (with $f'(\xi, \eta) > 0$ everywhere) are not possible for $w > 1/2$. However, they may not be possible even for values of $w < 1/2$ depending on the Lewis number. There are three possibilities.

(a) $Le = 1$. In this case, equation (25) reduces to

$$f'(\xi, \eta) = (1-2w)\theta(\xi, \eta) \equiv (1-2w)\phi(\xi, \eta). \tag{27}$$

When $w = 1/2$, the flow is zero everywhere (no flow). For $0 \leqslant w < 1/2$, the flow is upward since $f' > 0$ everywhere. For $1/2 < w \leqslant 1$, the flow is downward; the flow field for a given w value is identical to, but in the opposite direction to that for the $\langle 1-w \rangle$ value.

(b) $Le > 1$. For $Le > 1$, the concentration boundary layer is thinner than the thermal boundary layer; mathematically this implies that ϕ drops from unity at $\eta = 0$ to zero as $\eta \to \infty$ faster than does θ, i.e. $\phi(\xi, \eta) < \theta(\xi, \eta)$ throughout the boundary layer. Thus, for values of w between 0 and 1/2

$$w\phi(\xi, \eta) < (1-w)\theta(\xi, \eta).$$

Consequently, equation (25) shows that the prevailing thermal buoyancy effect in this case produces upward flows with $f'(\xi, \eta) > 0$ over the entire boundary region for $0 \leqslant w \leqslant 1/2$. It is even possible to obtain numerical solutions for w values slightly higher than $w > 1/2$: in these cases, the dominant thermal buoyancy effect produces an upward flow over most of the boundary region while the opposing solutal buoyancy effect, which is confined to the vicinity of the surface, causes a small downward flow next to the surface. However, such flows are contrary to the boundary layer assumption of no net flow at the leading edge and are therefore discarded. Similar observations on buoyant flows of Newtonian fluids have been noted by Gebhart and Pera [11].

(c) $Le < 1$. For $Le < 1$, the thermal boundary layer is thinner than the concentration boundary layer. The opposing solutal buoyancy effect dominates at the outer boundary region where $\phi(\xi, \eta) > \theta(\xi, \eta)$. Hence, equation (25) indicates that a flow reversal ($f' < 0$) will be manifest at the outer edge of the boundary layer for $w = 1/2$ (as well as for values of w less than, but generally close to 1/2 depending on the relative thickness of the thermal boundary layer). Thus for $Le < 1$, totally upward flows ($f' > 0$ everywhere) are not possible for the whole range $0 \leqslant w \leqslant 1/2$ but for a shorter range instead, represented by $0 \leqslant w \leqslant w^*$. The upper limit w^* varies between 0 and 1/2 as Le varies between 0 and 1. As in the $Le > 1$ case, it is

possible numerically to obtain predominantly upward flows with flow reversals in the outer part of the flow region for values of w in the range $w^* < w < 1/2$. Such flows are also discarded for the reason stated above.

4. NUMERICAL SOLUTIONS

Equations (19)–(22) were solved numerically by a finite-difference collocation scheme. In this method, the partial differential equations are first reduced to a set of ordinary differential equations by replacing the partial derivatives with respect to ξ by a finite-difference formula centered at the ξ-interval midpoint. The resulting set of ordinary differential equations are in turn reduced to an algebraic system by the collocation method. Specifically, cubic Hermite polynomials are used as interpolating functions which are forced to satisfy the differential equations at the Gaussian quadrature points. A graded η-spacing is used. The nonlinear system is solved recursively by the quasilinearization algorithm, using the converged solutions for the preceding ξ value as initial guesses for the current ξ value. The solution methodology is described in detail in ref. [12]. Solutions were carried out for Lewis numbers of 1, 2, 5, 10 and 100 and the transverse curvature parameter ξ ranging from 0 to 10. The buoyancy parameter w was varied between 0 and 1 for the aiding case, and between 0 and 1/2 for the opposing case, which is the valid range for $Le \geqslant 1$. The 'base case' solutions agree well with the local nonsimilarity solutions of Minkowycz and Cheng [9] for thermally driven flows. Recall that the 'base case' solutions are represented by

$$\theta(\xi,\eta;Le,0) \equiv \phi(\xi,\eta;Le,1) \equiv \theta(\xi,\eta;1,w) \equiv \phi(\xi,\eta;1,w)$$

and

$$f'(\xi,\eta;Le,0) \equiv f'(\xi,\eta;Le,1;\mathrm{AC}) \equiv -f'(\xi,\eta;Le,1:\mathrm{OC}) \equiv f'(\xi,\eta;1,w:\mathrm{AC}).$$

Although solutions were obtained only for $Le \geqslant 1$ in this study, the results and discussion presented in this section can be readily applied to cases with $Le \leqslant 1$ by taking advantage of the antisymmetry between the temperature and concentration equations in the present formulation. Equations (20)–(22) show that the temperature distribution $\theta(\xi,\eta)$ for a given set of $\langle Le, w\rangle$ values is identical to the concentration distribution $\phi(\xi,\eta)$ for the case with $\langle 1/Le, 1-w\rangle$ and vice versa, i.e.

$$\theta(\xi,\eta;Le,w) \equiv \phi(\xi,\eta;1/Le,1-w)$$

$$\phi(\xi,\eta;Le,w) \equiv \theta(\xi,\eta;1/Le,1-w).$$

Consequently, equation (19) shows that the flow field is invariant between these two cases

$$f'(\xi,\eta;Le,w) \equiv f'(\xi,\eta;1/Le,1-w).$$

In the aiding case, the above relations hold for all Le and $0 \leqslant w \leqslant 1$. In the opposing case, the above relations are valid for $Le \geqslant 1$ and $0 \leqslant w \leqslant 1/2$ (as well as for $Le < 1$ and $0 \leqslant w \leqslant w^*$);† however, the flow for $\langle 1/Le, 1-w\rangle$ is in the opposite (downward) direction as that for $\langle Le, w\rangle$. It should be noted that for downward flows, equation (25) is replaced by

$$f'(\xi,\eta) = -[(1-w)\theta(\xi,\eta) - w\phi(\xi,\eta)] \quad (28)$$

to account for the occurrence of flow in the negative x-direction.

Table 1 presents the temperature and concentration gradients at the surface for a vertical plate ($\xi = 0$). These values are related to the local Nusselt and Sherwood numbers by

$$Nu_x = q_w x/k(T_w - T_\infty) = (Gr_x/A)^{1/2}[-\theta'(\xi,0)] \quad (29a)$$

$$Sh_x = j_w x/D(T_w - T_\infty) = (Gr_x/A)^{1/2}[-\phi'(\xi,0)]. \quad (29b)$$

The variations of θ' and ϕ' with w are plotted in Fig. 2. In the aiding case, the heat transfer rates decrease with increasing w as the solutal buoyancy effect dominates. For $Le \geqslant 1$, the mass transfer rates are highest for heat transfer driven flow ($w = 0$); they increase with increasing values of Le which confines the concentration boundary layer to an increasingly thinner layer. In the opposing case, heat and mass transfer rates also decrease with w as the adverse concentration buoyancy effect impedes the upward flow.

Table 2 presents surface heat and mass transfer rates for a cylinder for selected values of ξ. Transverse curvature gives rise to higher temperature and concentration gradients at the surface. The relative increase in the heat and mass transfer rates due to curvature can be measured by the ratios of the local surface heat and mass flux along a vertical cylinder to

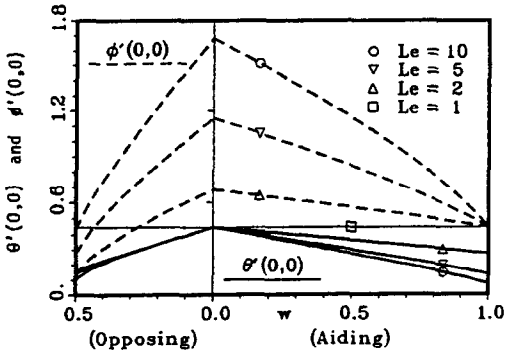

FIG. 2. Temperature and concentration gradients at the surface for $\xi = 0$ (vertical plate).

†Compared to the half range $0 \leqslant w \leqslant 1/2$ for $Le > 1$, upward flows for $Le < 1$ are possible for only a small range $0 \leqslant w \leqslant w^*$ ($w^* < 1/2$) and therefore are not presented in this study.

Table 1. Results for $A = -\theta'(0,0)$ and $B = -\phi'(0,0)$ for vertical plate

	$Le = 2$		$Le = 5$		$Le = 10$		$Le = 100$	
w	A	B	A	B	A	B	A	B
1.000 AC	0.275	0.444	0.134	0.444	0.073	0.444	0.011	0.444
0.833 AC	0.305	0.487	0.194	0.592	0.148	0.730	0.091	1.951
0.667 AC	0.335	0.529	0.249	0.720	0.213	0.956	0.165	2.836
0.500 AC	0.363	0.569	0.300	0.838	0.273	1.155	0.236	3.588
0.333 AC	0.390	0.608	0.350	0.948	0.332	1.339	0.306	4.275
0.167 AC	0.417	0.646	0.397	1.053	0.388	1.513	0.375	4.923
0.000	0.444	0.683	0.444	1.154	0.444	1.680	0.444	5.546
0.100 OC	0.392	0.601	0.391	1.004	0.392	1.458	0.396	4.805
0.167 OC	0.356	0.544	0.355	0.902	0.357	1.307	0.365	4.306
0.250 OC	0.308	0.468	0.309	0.770	0.313	1.114	0.325	3.671
0.333 OC	0.256	0.384	0.261	0.631	0.267	0.912	0.284	3.019
0.400 OC	0.208	0.308	0.219	0.510	0.228	0.740	0.251	2.473
0.450 OC	0.165	0.238	0.185	0.407	0.197	0.598	0.226	2.037
0.500 OC	0.102	0.136	0.141	0.277	0.160	0.427	0.199	1.550

AC, aiding case; OC, opposing case.

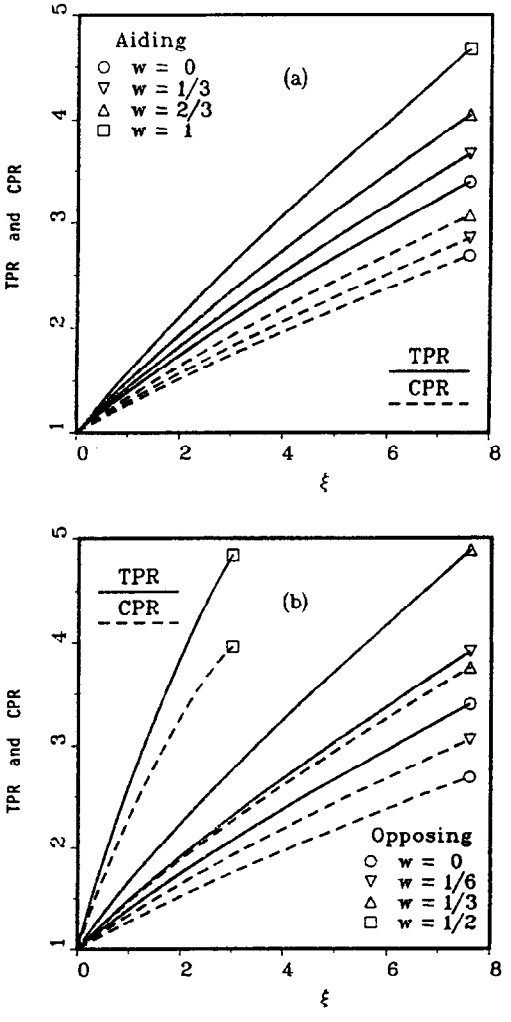

FIG. 3. Heat and mass transfer rates for $Le = 2$: (a) aiding case; (b) opposing case.

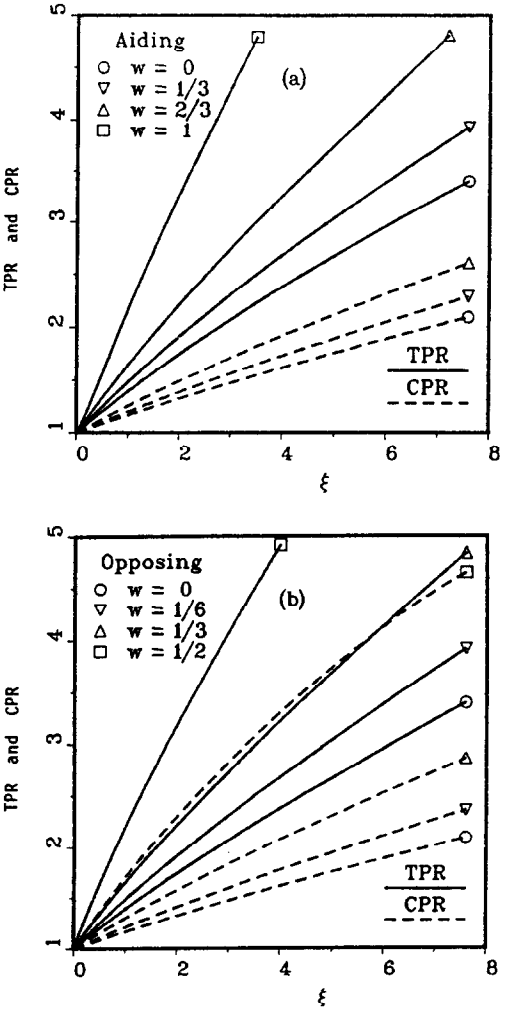

FIG. 4. Heat and mass transfer rates for $Le = 5$: (a) aiding case; (b) opposing case.

Table 2. Results for $A = -\theta'(\xi, 0)$ and $B = -\phi'(\xi, 0)$ for vertical cylinder

	$Le = 2$		$Le = 5$		$Le = 10$		$Le = 100$	
w	A	B	A	B	A	B	A	B
			(a) $\xi = 1$					
1.000 AC	0.435	0.619	0.290	0.619	0.242	0.619	0.203	0.619
0.833 AC	0.469	0.665	0.349	0.774	0.301	0.915	0.245	2.143
0.667 AC	0.502	0.709	0.410	0.906	0.372	1.145	0.324	3.033
0.500 AC	0.533	0.751	0.466	1.026	0.439	1.347	0.401	3.787
0.333 AC	0.562	0.792	0.520	1.139	0.501	1.533	0.476	4.476
0.167 AC	0.591	0.831	0.570	1.245	0.561	1.709	0.548	5.126
0.000	0.619	0.869	0.619	1.348	0.619	1.878	0.619	5.750
0.167 OC	0.529	0.728	0.529	1.095	0.531	1.504	0.538	4.511
0.333 OC	0.427	0.566	0.433	0.823	0.439	1.110	0.455	3.227
0.500 OC	0.268	0.313	0.310	0.473	0.330	0.633	0.366	1.774
			(b) $\xi = 2$					
1.000 AC	0.581	0.775	0.437	0.775	0.391	0.775	0.352	0.775
0.833 AC	0.615	0.824	0.490	0.937	0.440	1.083	0.385	2.327
0.667 AC	0.650	0.870	0.551	1.076	0.510	1.321	0.460	3.225
0.500 AC	0.683	0.915	0.612	1.200	0.582	1.528	0.543	3.984
0.333 AC	0.714	0.957	0.669	1.315	0.649	1.718	0.623	4.676
0.167 AC	0.745	0.998	0.723	1.425	0.714	1.896	0.700	5.328
0.000	0.775	1.038	0.775	1.530	0.775	2.067	0.775	5.953
0.167 OC	0.681	0.893	0.681	1.274	0.683	1.692	0.690	4.715
0.333 OC	0.572	0.724	0.580	0.997	0.586	1.294	0.602	3.434
0.500 OC	0.395	0.447	0.449	0.638	0.470	0.814	0.508	1.994
			(c) $\xi = 5$					
1.000 AC	0.973	1.187	0.834	1.187	0.791	1.187	0.755	1.187
0.833 AC	1.008	1.242	0.879	1.369	0.833	1.531	0.782	2.841
0.667 AC	1.044	1.296	0.934	1.526	0.889	1.794	0.834	3.770
0.500 AC	1.080	1.347	0.998	1.666	0.963	2.020	0.919	4.549
0.333 AC	1.117	1.396	1.063	1.794	1.040	2.224	1.011	5.255
0.167 AC	1.152	1.443	1.126	1.913	1.115	2.414	1.100	5.916
0.000	1.187	1.488	1.187	2.027	1.187	2.595	1.187	6.549
0.167 OC	1.080	1.327	1.080	1.756	1.083	2.206	1.090	5.310
0.333 OC	0.952	1.132	0.963	1.457	0.971	1.790	0.989	4.028
0.500 OC	n/c	n/c	0.805	1.035	0.836	1.265	0.882	2.594
			(d) $\xi = 10$					
1.000 AC	1.563	1.787	1.435	1.787	1.397	1.787	1.364	1.787
0.833 AC	1.597	1.849	1.478	1.994	1.438	2.180	1.389	3.613
0.667 AC	1.632	1.911	1.524	2.177	1.481	2.482	1.425	4.597
0.500 AC	1.670	1.971	1.580	2.341	1.542	2.741	1.493	5.415
0.333 AC	1.708	2.029	1.647	2.490	1.621	2.971	1.586	6.149
0.167 AC	1.748	2.085	1.717	2.628	1.704	3.183	1.687	6.832
0.000	1.787	2.139	1.787	2.757	1.787	3.381	1.787	7.482
0.167 OC	1.662	1.948	1.664	2.456	1.667	2.964	1.676	6.232
0.333 OC	1.513	1.705	1.529	2.109	1.540	2.502	1.563	4.929
0.500 OC	n/c	n/c	n/c	n/c	1.389	1.854	1.454	3.446

AC, aiding case; OC, opposing case; n/c no convergence.

those for a vertical plate. These are given by

$$TPR = [q_w(x)]_{cyl}/[q_w(x)]_{pl} = [-\theta'(\xi, 0)]/[-\theta'(0, 0)] \quad (30a)$$

$$CPR = [j_w(x)]_{cyl}/[j_w(x)]_{pl} = [-\phi'(\xi, 0)]/[-\phi'(0, 0)]. \quad (30b)$$

The ratios TPR and CPR are plotted against ξ in Figs. 3 and 4. Overall, the ratios increase nonlinearly at first but linearly for higher ξ values. The relative increase in the heat flux is particularly strong for w values close to 1 in the aiding case and for w values close to 1/2 in the opposing case. This is also true for the mass flux in the latter case.

Representative temperature and concentration profiles are presented in Fig. 5 for $Le = 2$ and in Fig. 6 for $Le = 10$. Temperature and concentration variations monotonically decrease from a maximum value of 1 at the surface to 0 at infinity. The effect of transverse curvature (ξ) is to sharpen the variations near the surface but flatten the variations in the outer region, resulting in thicker boundary layers. The temperature boundary layer thickness δ_T and the concentration boundary layer thickness δ_C also increase with increasing w in both aiding and opposing cases. In the aiding

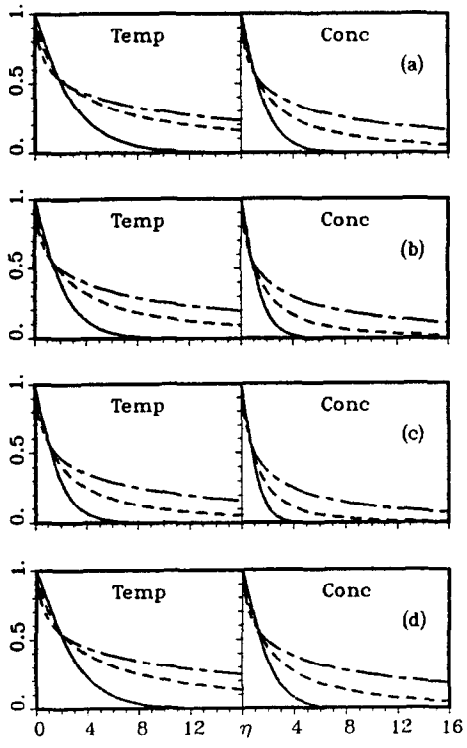

FIG. 5. Dimensionless temperature and concentration profiles for $Le = 2$: (a) $w = 1$ AC; (b) $w = 1/2$ AC; (c) $w = 0$; (d) $w = 1/3$ OC (———, $\xi = 0$; – – –, $\xi = 2$; —·—, $\xi = 10$).

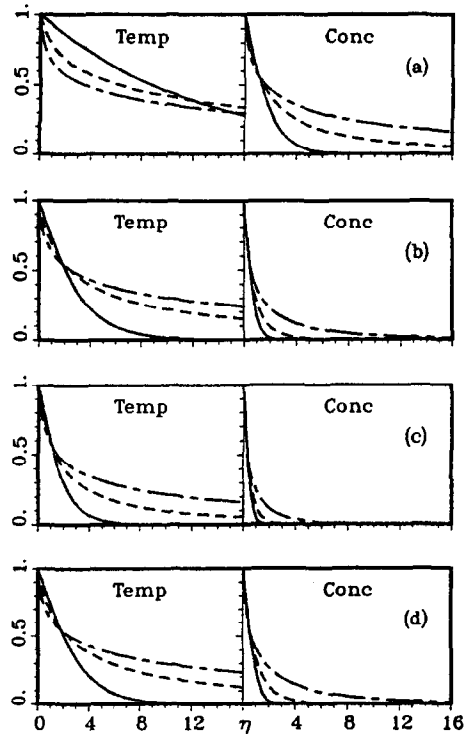

FIG. 6. Dimensionless temperature and concentration profiles for $Le = 10$: (a) $w = 1$ AC; (b) $w = 1/2$ AC; (c) $w = 0$; (d) $w = 1/3$ OC (———, $\xi = 0$; – – –, $\xi = 2$; —·—, $\xi = 10$).

case, δ_T increases with increasing Le, while δ_C decreases since the concentration variations are confined to thinner layers as the Lewis number is increased. In the opposing case, the influence of Le on the temperature distribution is negligible except for w values close to 1/2.

The characteristics of the possible flow regimes are illustrated in Fig. 7 for both aiding and opposing cases. In the aiding case, the resultant velocity variations are also monotonically decreasing from a maximum value of 1 at the surface to 0 at infinity. Since the limiting flows for $w = 0$ and 1 are identical, the velocity profiles initially diverge from, but later converge to these 'base case' solutions. The maximum deviation from the base case solutions occurs around $w = 1/2$ shifting towards $w = 1$ as Le increases. The velocity gradients become steeper near the surface but become flatter away from it with increasing curvature parameter ξ, which increases the boundary layer thickness.

In the opposing case, the upward flow is weakened considerably by the counteracting solutal buoyancy forces. Velocity profiles for $Le = 1$ are still monotonically decreasing from a maximum value of $f' = 1 - 2w$ at the surface. For $Le > 1$, however, velocities near the surface can overshoot this value as w is increased. Thus the maximum velocity moves into the boundary layer beyond a threshold w value for a given Le. This threshold value is smaller for higher Le values. For a given w, the magnitude of the velocity overshoot increases with Le. The effect of curvature is to suppress or reduce this tendency and displace it away from the surface.

5. SUMMARY

A global treatment of heat and mass transfer in free convection about a vertical planar or cylindrical surface in a saturated porous medium is presented. Boundary layer analysis is formulated such that the governing equations can predict the whole spectrum of flows ranging from purely heat transfer driven flow to purely mass transfer driven flow. To this end, a buoyancy parameter w representing the magnitude of the solutal buoyancy force relative to the combined buoyancy force is introduced. Numerical solutions are generated for Lewis numbers 1, 2, 5, 10 and 100. When the solutal density gradient assists the thermal density gradient, upward flows (positive everywhere) are possible for the full range $0 \leqslant w \leqslant 1$ for any value of the Lewis number. For cases with adverse solutal density gradients, upward flows are possible for the half range $0 \leqslant w \leqslant 1/2$ when $Le \geqslant 1$ and for an even shorter w range when $Le < 1$. The curvature of the cylinder increases the surface heat and mass transfer rates and leads to thicker boundary layers. Although numerical results are presented for $Le \geqslant 1$ and upward flows only, they can be readily applied to cases with $Le < 1$ and/or to downward flows by taking

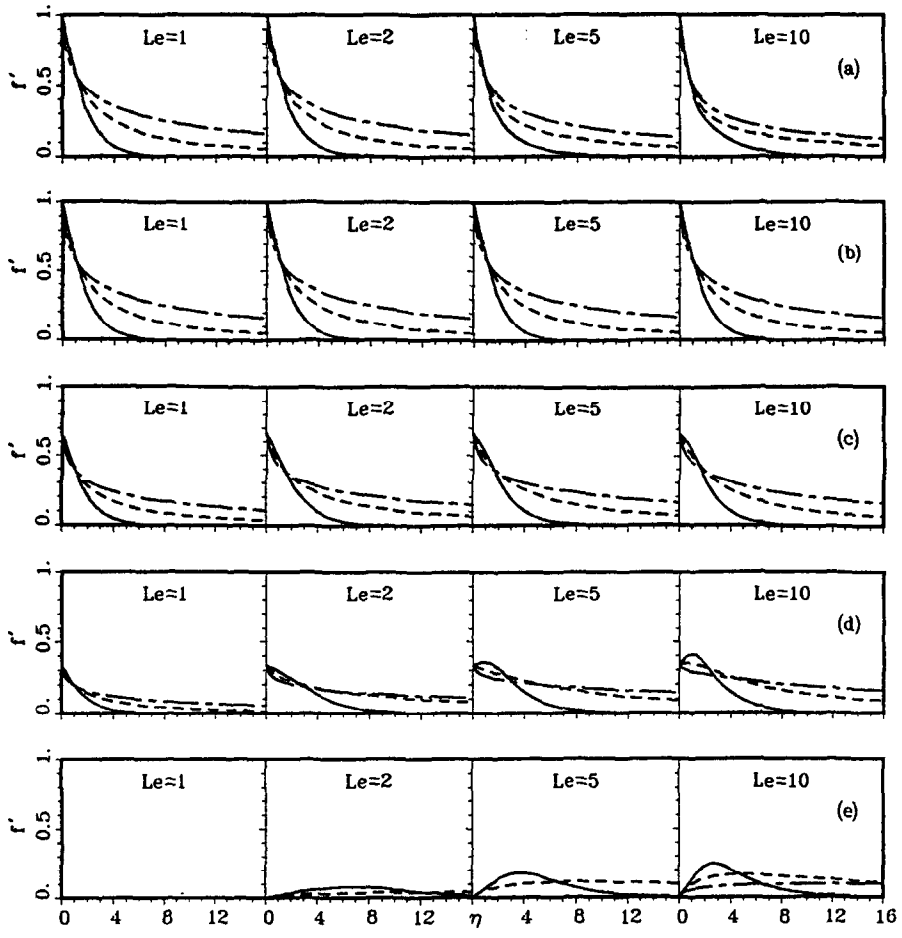

FIG. 7. Dimensionless velocity (f') profiles for $Le = 1, 2, 5$ and 10: (a) $w = 1/2$ AC; (b) $w = 0$; (c) $w = 1/6$ OC; (d) $w = 1/3$ OC; (e) $w = 1/2$ OC (———, $\xi = 0$; – – –, $\xi = 2$; — · —, $\xi = 10$).

advantage of the antisymmetry property in the formulation of the problem.

REFERENCES

1. P. Cheng, Geothermal heat transfer. In *Handbook of Heat Transfer Applications* (Edited by W. M. Rohsenow *et al.*) 2nd Edn, Chap. 11. McGraw-Hill, New York (1985).
2. F. A. Kulacki and M. Keyhani, Heat transfer aspects of nuclear waste disposal. In *Heat Transfer Problems in Nuclear Waste Management* (Edited by E. V. McAssey, Jr. and V. E. Schrock), HTD-Vol. 67, pp. 1–17. ASME, New York (1987).
3. D. A. Nield, Onset of thermohaline convection in a porous medium, *Water Resour. Res.* **4**, 553–560 (1968).
4. G. Z. Gershuni, E. M. Zukhovitskii and D. Y. Lyubimov, Thermal concentration instability of a mixture in a porous medium, *Sov. Phys. Dokl.* **21**, 375–377 (1976).
5. J.-Y. Yang and W.-J. Chang, The flow and vortex instability of horizontal natural convection in a porous medium resulting from combined heat and mass buoyancy effects, *Int. J. Heat Mass Transfer* **31**, 769–777 (1988).
6. A. Bejan and K. R. Khair, Heat and mass transfer by natural convection in a porous medium, *Int. J. Heat Mass Transfer* **28**, 909–918 (1985).
7. O. V. Trevisan and A. Bejan, Natural convection with combined heat and mass transfer buoyancy effects in a porous medium, *Int. J. Heat Mass Transfer* **28**, 1597–1611 (1985).
8. D. G. Evans and J. A. Nunn, Free thermohaline convection in sediments surrounding a salt column, *J. Geophys. Res.* **94**, 12413–12422 (1989).
9. W. J. Minkowycz and P. Cheng, Free convection about a vertical cylinder embedded in a porous medium, *Int. J. Heat Mass Transfer* **19**, 805–813 (1976).
10. D. B. Ingham and I. Pop, A horizontal flow past a partially heated infinite vertical cylinder embedded in a porous medium, *Int. J. Engng Sci.* **24**, 1351–1363 (1986).
11. B. Gebhart and L. Pera, The nature of vertical natural convection flows resulting from the combined buoyancy effects of thermal and mass diffusion, *Int. J. Heat Mass Transfer* **14**, 2025–2050 (1971).
12. A. Yücel, The influence of injection or withdrawal of fluid on free convection about a vertical cylinder in a porous medium, *Numer. Heat Transfer* **7**, 483–493 (1984).

CONVECTION NATURELLE DE CHALEUR ET DE MASSE LE LONG D'UN CYLINDRE VERTICAL DANS UN MILIEU POREUX

Résumé—On étudie la convection naturelle simultanée de chaleur et de masse le long d'un cylindre dans un milieu poreux. L'analyse de couche limite est formulée en fonction de l'effet de flottement thermique et solutal. Les caractéristiques du champ d'écoulement sont analysées en détail pour les deux cas où les gradients de concentration sont soit aidés soit contrariés par les forces de flottement thermique. On discute les effets de la courbure, du paramètre de flottement et du nombre de Lewis sur les champs de température de concentration et de vitesse et sur les flux de chaleur et de masse à la surface.

WÄRME- UND STOFFÜBERTRAGUNG BEI NATÜRLICHER KONVEKTION AN EINEM SENKRECHTEN ZYLINDER IN EINEM PORÖSEN MEDIUM

Zusammenfassung—Der gekoppelte Wärme- und Stofftransport bei natürlicher Konvektion an einem senkrechten Zylinder in einem gesättigten porösen Medium wird untersucht. Bei der Formulierung der Grenzschichtgleichungen werden die gekoppelten Auftriebseffekte durch Dichte- und Konzentrationsunterschiede berücksichtigt. Die Strömungsfelder werden für den Fall gleichgerichteter wie auch für den Fall entgegengesetzt wirkender Auftriebskräfte durch Konzentrations- und Dichteunterschiede detailliert untersucht. Die Einflüsse der Krümmung, des Auftriebsparameters und der Lewis-Zahl auf das Temperatur-, Konzentrations- und Strömungsfeld sowie auf den Wärme- und Stofftransport an der Oberfläche werden diskutiert.

ЕСТЕСТВЕННОКОНВЕКТИВНЫЙ ТЕПЛО- И МАССОПЕРЕНОС ВДОЛЬ ВЕРТИКАЛЬНОГО ЦИЛИНДРА, ПОМЕЩЕННОГО В ПОРИСТУЮ СРЕДУ

Аннотация—Исследуется совместный естественноконвективный тепло- и массоперенос вдоль вертикального цилиндра, помещенного в насыщенную пористую среду. Задача пограничного слоя формулируется на основе теплового и концентрационного эффектов плавучести. Характеристики поля течения анализируются для двух случаев, когда градиенты концентрации действуют либо против, либо совместно с тепловой подъемной силой. Анализируется влияние кривизны, параметра подъемной силы и числа Льюиса на поля температуры, концентрации и течения, а также на коэффициенты тепло- и массопереноса на поверхности.